

BRNO UNIVERSITY OF TECHNOLOGY

Faculty of Mechanical Engineering

Institute of Solid Mechanics

Ing. Roman Gröger

**CHARACTERIZATION OF FRACTURE-MECHANICAL
BEHAVIOR OF BIMATERIAL V-NOTCHES USING BEM**

**POPIS LOMOVĚ-MECHANICKÉHO CHOVÁNÍ
BIMATERIÁLOVÝCH V-VRUBŮ POMOCÍ BEM**

SHORT VERSION OF PH.D. THESIS

Study field: Engineering Mechanics

Supervisor: Prof. RNDr. Zdeněk Knésl, CSc. (ÚFM AV ČR, Brno)

Opponents: Prof. RNDr. Michal Kotoul, DrSc. (ÚMT, FSI, VUT Brno)
Prof. RNDr. Vladimír Sládek, DrSc. (ÚSTARCH SAV, Bratislava)

Presentation date: August 27, 2003

KEYWORDS

V-notch, bimaterial interface, boundary elements, layered structure, generalized stress intensity factor, T-stress, stability criterion.

KLÍČOVÁ SLOVA

V-vrub, bimateriálové rozhraní, hraniční prvky, vrstvený materiál, zobecněný faktor intenzity napětí, T-napětí, kritérium stability.

PLACE OF STORAGE

The Dissertation is stored at the Department of Science and Research, Faculty of Mechanical Engineering, Brno University of Technology, Technická 2, 616 69 Brno.

© Roman Gröger, 2000-2003

Institute of Solid Mechanics, Faculty of Mechanical Engineering Brno University of Technology,
Technická 2, 616 69 Brno, Czech Republic

and

Institute of Physics of Materials, Academy of Sciences of the Czech Republic
Žižkova 22, 616 62 Brno, Czech Republic

ISBN 80-214-2473-7

ISSN 1213-4198

CONTENTS

1	INTRODUCTION	5
2	PRESENT STATE OF THE RESEARCH	6
3	MAIN AIMS OF THE WORK	6
4	ANALYTICAL EXPRESSION OF THE STRESS FIELD	7
4.1	Stress field around a V-notch tip	7
4.2	Fracture-mechanical parameters and their physical meaning	10
5	QUANTIFICATION OF THE FRACTURE-MECHANICAL PARAMETERS	11
5.1	Extrapolation of the GSIF and T-stress	11
5.2	Integral approach to the calculation of the GSIF	13
5.3	On the calculation of T-stresses using the contour integrals	14
5.4	Assessment of the stability of bimaterial V-notches	15
6	INTRODUCTION TO THE BOUNDARY ELEMENT METHOD	17
6.1	Governing equation of elastostatics	17
6.2	Calculation of internal displacements	18
6.3	Integral representation of internal stresses	19
6.4	Numerical treatment at corner points	20
7	EXAMPLES	22
7.1	Simulation of the tension experiment	22
7.2	A notch perpendicular to bimaterial interface	24
7.3	Inclined notch terminating at the interface	28
8	CONCLUSION	31
	REFERENCES	32
	AUTHOR'S CURRICULUM VITAE	33

Abstrakt

Předložená práce uvádí teoretický model pro hodnocení stability bimateriálových V-vrubů vznikajících na povrchu křehkých materiálů. V důsledku zvýšených napětí v okolí těchto koncentrátorů napětí je možná iniciace mikrotrhliny a její další šíření v závislosti na charakteru vnějšího namáhání. Dosáhne-li hustota deformační energie hodnoty potřebné pro růst trhliny, dochází v případě křehkých materiálů téměř okamžitě k nestabilnímu růstu trhliny a delaminaci zbytkového průřezu. V opačném případě je nestabilitě zamezeno; rozhraní pak působí jako překážka k šíření trhliny a v některých případech lze dokonce pozorovat i zastavení trhliny na tomto rozhraní.

Uvažujeme-li lineárně-elastické chování všech oblastí modelu, lze pro popis napětově-deformačních stavů použít lineárně-elastickou lomovou mechaniku. Pole napětí v okolí obecně orientovaného bimateriálového V-vrubu lze analyticky vyjádřit ve tvaru nekonečné řady, tzv. *Williamsova řešení*. Každý člen tohoto rozvoje je jednoznačně definován svým vlastním číslem λ , vlastní funkcí $f(\lambda, \theta)$ a radiálním členem tvaru $r^{\lambda-1}$. V blízkosti kořene V-vrubu tak zřejmě vymizí ty členy rozvoje, kterým přísluší vlastní číslo $\lambda > 1$. Naopak napětové členy odpovídající $\lambda \leq 0$ způsobují divergenci energie napjatosti, v důsledku čehož je nutné tyto členy vyjmout z Williamsova rozvoje. Pole napětí v okolí obecného bimateriálového V-vrubu je tak zřejmě možné popsat konečným počtem členů Williamsova rozvoje, z nichž napětové členy odpovídající vlastním číslům $0 < \lambda < 1$ jsou nazývány jako *singulární* a pro $\lambda = 1$ mluvíme o *nesingulárním* členu rozvoje napětí. Hodnoty příslušných koeficientů, až na amplitudy napětových členů, které se přímo vztahují k tzv. *lomově-mechanickým parametrům*, je možné stanovit řešením systému algebraických rovnic.

Pro kvantifikaci zbývajících lomově-mechanických parametrů je zapotřebí znalosti celého pole napětí, které je v obecném případě získáno numericky. Výpočtový model byl sestaven z konečného počtu tzv. *hraničních prvků*, které jednoznačně určují tvar modelované součásti. Deformační a silové okrajové podmínky byly předepsány pouze na hranici a s použitím izoparametrických tvarových funkcí transformovány do uzlů jednotlivých prvků. Hledané posuvy a napětí v uzlech hranice lze pak určit s využitím příslušné hraniční integrální rovnice.

Výpočet lomově-mechanických parametrů ze znalosti pole napětí je možný buď přímou nebo integrální cestou, přičemž obě metody jsou v Disertační práci modifikovány pro aplikaci na bimateriálové V-vrubu. Integrální model výpočtu je založen na platnosti Bettiho recipročního teorému definovaného mezi dvěma nezávislými elastickými stavy, z nichž jeden odpovídá dané úloze a druhým je analyticky vyjádřitelné pomocné řešení splňující stejné okrajové podmínky jako řešená úloha.

Posuzování stability obecného koncentrátoru napětí je třeba provádět na základě vhodného kritéria stability trhliny. Jedním z možných a fyzikálně podložených přístupů je známé Sihovo kritérium hustoty deformační energie. Toto kritérium bylo v předložené práci modifikováno tak, aby zahrnovalo všechny singulární a také nesingulární napětové členy přítomné ve Williamsově rozvoji. Bimateriálový V-vrub je pak chápán jako stabilní v případě, kdy je hodnota Sihova faktoru menší než jeho kritická velikost, která je materiálovou charakteristikou.

Konkrétní výpočty byly provedeny na homogenních i bimateriálových tělesech porušených ostrou trhlinou i různě orientovanými V-vrubu dosahujícími bimateriálového rozhraní. Ukázáno je také kvantitativní srovnání integrálního přístupu s hodnotami získanými přímou extrapolací metodou. U bimateriálových těles je navíc vyjádřen modifikovaný Sihův faktor a směr šíření mikrostrukturální trhliny, iniciované v kořeni V-vrubu, do cílového materiálu.

1 INTRODUCTION

Many successful wear resisting materials consist of a thin layer of ceramic on a thicker metallic substrate. These layered structures are conveniently made using the laser beam with the high energy density, which is capable of melting the metallic substrate and partly also the ceramic powder resulting in solid bonding between the ceramic and the metal. However, as the physical properties between ceramic and metallic materials are vastly different, e.g. coefficient of thermal expansion and crystallographic structures, cracks usually develop at the interface as well as inside the rapidly solidified layer. This process of thermal bonding was previously used by De Hosson *et al* for the study of coating a duplex steel SAF 2205, stainless steel 304 and Fe-22 wt% Cr. Similar analysis of interface made of a mixture of SiO₂ and Al powder injected in the laser-melted surface of aluminium was published recently [4].

Mathematical description of the stress field and associated theories dealing with the stability of cracks in layered structures are rather well investigated. Although this continuum-level description cannot explain the processes and interactions in the micro-level, such results are still very important for engineering practice. Because the associated mathematical apparatus quantifying the stability of the crack-like flaws in homogeneous materials is widely accepted, this so-called limit analytical solution becomes very popular among engineers and materials scientists.

To make this theory applicable to a broader class of stress concentrators, let us start with the simpler two-parameter linear-elastic fracture mechanics. The stress field around a sharp crack can be analytically expressed by using the so-called Williams eigenfunction expansion that is a solution to the biharmonic partial differential equation of elastostatics. Some of the resulting stress terms included in the Williams series exhibit a strong singular dependence on the radial distance as the internal point approaches the crack tip. Moreover, also the stress term independent of the radial coordinate is always solution to the this differential equation. The two-parameter description then states that a reasonably accurate continuum description of the stress field around such a crack tip should involve all the singular stress terms proportional to r^{-p} (p is the stress singularity exponent) and also the nonsingular field ($p = 0$). Once the amplitudes of the stress fields are quantified, the stress field around the analyzed flaw is uniquely mapped. These unknown coefficients are commonly called as the *fracture-mechanical parameters*. Particularly, the coefficients belonging to the singular stress fields are referred to as the *stress intensity factors* (SIF), whereas the nonsingular stress term is governed by the elastic *T-stress*. It is then assumed that the sudden brittle failure occurs when the combined effect of the SIF and T-stress falls into the so-called *fracture toughness locus* [6]. This locus can be measured experimentally on a set of specimens and we can therefore regard the fracture toughness locus as the material characteristic.

Since the mechanical parts are made of two or more layers of elastic materials, e.g. hard, wear-resistant ceramic coating deposited on a more compliant substrate, it is necessary to investigate the conditions under which these bimetals failure. The interface between the two layers is mostly modeled as bonded with the continuity of displacements and equilibrium of tractions along the joint. Therefore, one should be careful with applying this method to materials, where a significant slip between coating and substrate can be expected. Apparently, in these cases the real behavior and also the nature of crack propagation is affected mainly by the microstructural properties of the interface.

A further generalization can be made if a crack emanating from an arbitrarily open V-notch is assumed. This can be practically observed in almost every area of engineering. The surface

scratches or cracks give birth to an elevated stress field in a vicinity of their tips and, if the strength of the stress field is high enough, the growth of the microscopic cracks initiated within the plastic zone ahead of the V-notch tip is allowed. The crack growth can be very rapid and the consequences of the brittle failure are often catastrophic. It is therefore paramount to understand the processes associated with such a failure and introduce a sufficiently accurate numerical procedure for the prediction of the onset of brittle failure.

2 PRESENT STATE OF THE RESEARCH

In the ceramic coating, the cracks are usually observed in thermally-affected zone just outside the laser track [4] and often aligned perpendicularly to the interface. To maintain the structural integrity of such bimetals, it is necessary to predict how these cracks will interact with the interface. i.e. whether they propagate into the substrate or will cause a delamination of the interface itself.

Analytical theory describing the stress and displacement field around an arbitrarily oriented crack meeting an interface was introduced by Fenner [5] and Bogy [3]. They showed that the Williams eigenfunction expansion has generally two singular stress terms corresponding to two different eigenvalues λ . Since the stress singularity exponent defined as $p = 1 - \lambda$ is now variable and falls into $0 < p < 1$, the corresponding amplitudes of the singular stress terms are called as the *generalized stress intensity factors* (GSIF). Methods for the quantification of such parameters can be distinguished as:

- **extrapolation methods** – stress or displacement field is determined numerically, mostly using the Finite Element Method (FEM) or by the Boundary Element Method (BEM). The known stress or displacement components are then substituted into their analytical expressions and the corresponding SIF or GSIF is extrapolated into the crack tip as the intercept of the regression line [12].
- **contour integral methods** – based on the path-independent integrals, where two configurations satisfying the same boundary conditions are used. First state is the actual stress state in the body with unknown SIF or GSIF, whereas the latter is the auxiliary solution that has to be known analytically. The equilibrium between these two configurations is attained in the sense of the Betti reciprocal theorem [13].

Similar methods are also applicable to the calculation of the elastic T-stress. However, several differences should be recognized between the quantification of the amplitudes of the singular stress fields and nonsingular fields. Firstly, the extrapolation of the T-stress is often carried out on the basis of the singular stress terms. This apparently means that, to be able to obtain the extrapolated value of the T-stress, one has to first determine the corresponding SIFs or GSIFs. Secondly, despite its great applicability to cracks in homogeneous bodies and also to interface cracks [15], the contour integral method was not yet fully developed for the quantification of the T-stress for cracked bimetals, where the crack or V-notch type flaw terminates at the interface joining the two elastic layers.

3 MAIN AIMS OF THE WORK

Although, much work has been already done in attempt to predict the behavior of V-notches under external loading, some parts of the theory are still not fully consistent. The main

problem is associated with the quantification of the fracture-mechanical parameters that are directly related to the stability of the notches. The first goal of this Dissertation is therefore associated with the development of a sufficiently accurate numerical procedure that would be capable of determining the fracture-mechanical parameters for any type of geometry and orientation of the V-notch towards the bimaterial interface.

Another problem is the decision on the stability of the bimaterial cracks and V-notches. Since the GSIFs calculated for a particular configuration are not appropriate for direct comparison due to their dimensional dependence on the magnitude of the corresponding eigenvalues (H [MPa.m^{1-λ}]), one has to make this assessment on indirect basis. One of the feasible and physically consistent ways to attain this goal is to generalize the standard Sih's strain energy density criterion to account for both the GSIFs and the T-stress. The modified strain energy density factor Σ would then be an unambiguous quantity that could be directly compared with its critical value Σ_C to decide on the stability of the analyzed flaw.

The common feature of every continuum model of linear-elastic fracture mechanics is the necessary knowledge of the stress and displacement field around the analyzed defect. This is often achieved by using the Finite Element Method that calculates the stress tensor at every node inside the model and on the boundary. However, since we are primarily interested in the neighborhood of the crack or notch tip, a vast majority of information obtained from FEM is redundant in our fracture-mechanical considerations. To obtain the stress field of a large, geometrically complex model, the finite element mesh would need to be reasonably refined to reflect the nature of wedges, corners, notches, cracks, etc. The number of algebraic equations and the computational difficulty associated with the numerical solution of these huge systems is obvious.

To make the decisions on the stability of flaws more compact, one can use for example the Boundary Element Method that discretizes only the boundary of the model. In this method, the unknown magnitudes of displacements and tractions at the boundary are determined exactly. Furthermore, the internal stresses and displacements are calculated only at the points of interest by using the appropriate integral representation. In comparison to the linear FEM, the elastostatic Boundary Element Method is more mathematically complex, which is probably the reason why it has not been as widely accepted as the FEM. Nevertheless, the advantage of BEM over other methods for the solution of fracture-mechanical problems is undoubted. The study and thorough understanding of the underlying theory of BEM and algorithms of the calculation of internal stresses and displacements were therefore the other steps to the successful application of this method.

4 ANALYTICAL EXPRESSION OF THE STRESS FIELD

4.1 Stress field around a V-notch tip

To present the analytical description of the stress and displacement field around a V-notch tip arbitrarily oriented towards the bimaterial interface, let us assume that both layers are homogeneous, isotropic and with linear-elastic behavior. We are interested here in two-dimensional problems with either plane strain or plane stress condition.

According to the Theory of elasticity [17] the equilibrium in a 2-D elastic body is governed by the biharmonic partial differential equation

$$\Delta\Delta\Phi_i = 0 \quad , \quad (1)$$

where Δ is the Laplace operator and Φ_i is a particular stress function corresponding to domain i of the model. Let us assume that the model consists of three elastic domains, as shown in Fig. 1, addressed by $i = 1, 2, 3$ with generally dissimilar elastic properties. The solution to this differential equation is expressed in the form of the Williams eigenfunction expansion:

$$\Phi_i = \sum_{k=1}^{\infty} A_k r^{\lambda_k+1} F_{ik}(\theta, \lambda_k) \quad , \quad (2)$$

where A_k are the unknown coefficients, λ_k are eigenvalues, F_{ik} are eigenfunctions, and r, θ are the usual polar coordinates. Although the expression (2) is not terminated, the only term $\Phi_i = Ar^{\lambda+1}F_i(\theta, \lambda)$, where $\lambda \in (0;1)$, is usually taken into account for the so-called *limit analytical solution* (subscript index $k = 1$ is omitted when referring to this first term).

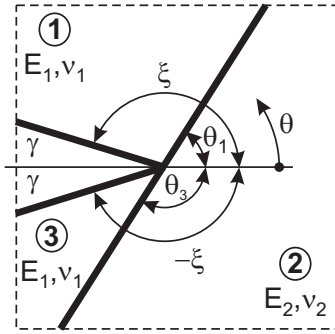


Figure 1: A notch terminating at interface between two dissimilar materials.

Differentiating the stress function Φ_i and substituting into (1), one can achieve the fourth-order ordinary differential equation for the calculation of eigenfunction F_i :

$$F_i^{(4)} + 2(1 + \lambda^2)F_i'' + (1 - \lambda^2)^2F_i = 0 \quad , \quad (3)$$

where prime denotes the derivative with respect to the angular coordinate θ . The characteristic equation of (3) has two complex-conjugate roots. The overall solution can then be expressed as a sum of two even cosine functions and two odd sine functions as

$$F_i(\theta, \lambda) = a_i \sin(\lambda + 1)\theta + b_i \cos(\lambda + 1)\theta + c_i \sin(\lambda - 1)\theta + d_i \cos(\lambda - 1)\theta \quad , \quad (4)$$

where a_i, b_i, c_i, d_i are unknown constants. Now, in view of Eq. (2), we have thirteen unknown parameters, twelve of them a_i, b_i, c_i, d_i for $i = 1, 2, 3$ and the eigenvalue λ . It will subsequently be shown that the numerical analysis of the entire model with prescribed boundary conditions is needed to fully describe the stress state in the body.

The polar stress components of the stress field around a V-notch tip can be obtained by differentiating the stress function Φ_i . For a specific domain i of the model, the stress field can be written as

$$\begin{aligned} \sigma_{irr} &= Ar^{\lambda-1} [F_i'' + (\lambda + 1)F_i] \\ \sigma_{i\theta\theta} &= Ar^{\lambda-1} [\lambda(\lambda + 1)F_i] \\ \sigma_{ir\theta} &= Ar^{\lambda-1} [-\lambda F_i'] \quad . \end{aligned} \quad (5)$$

It is apparent that the stress field resembles a singular behavior with respect to radial distance r for all eigenvalues $0 < \lambda < 1$ and nonsingular behavior for $\lambda = 1$. Applying the Hooke's law on the set (5), the corresponding polar displacements can be expressed as

$$\begin{aligned} u_{ir} &= A \frac{r^\lambda}{2\mu_i} \left\{ -(\lambda + 1)F_i + \frac{1 - \bar{\nu}_i}{\lambda} [F_i'' + (\lambda + 1)^2 F_i] \right\} \\ u_{i\theta} &= A \frac{r^\lambda}{2\mu_i} \left\{ -F_i' - \frac{1 - \bar{\nu}_i}{\lambda(\lambda - 1)} [F_i''' + (\lambda + 1)^2 F_i'] \right\} \quad , \end{aligned} \quad (6)$$

where $\bar{\nu}_i = \nu_i$ for plane strain, $\bar{\nu}_i = \nu_i/(1 + \nu_i)$ for plane stress, and ν_i is the Poisson's ratio of domain i .

Now we focus on the solution of the thirteen unknown parameters introduced above. Let us denote γ the half notch angle and $\xi = \pi - \gamma$ the complement angle, as shown in Fig. 1. Providing that the notch faces are traction-free, the following set of constraints along the notch faces has to be satisfied:

$$\sigma_{1\theta\theta}(r, \xi) = \sigma_{1r\theta}(r, \xi) = \sigma_{3\theta\theta}(r, -\xi) = \sigma_{3r\theta}(r, -\xi) = 0 \quad , \quad (7)$$

where the first subscript denotes the material to which a particular component corresponds. Consider that the interface between material 1 and 2 and also between 3 and 2 is perfectly bonded or welded, in other words. The following set of displacement pairs is then required along the interface:

$$\begin{aligned} u_{1r}(r, \theta_1) &= u_{2r}(r, \theta_1) \\ u_{1\theta}(r, \theta_1) &= u_{2\theta}(r, \theta_1) \\ u_{3r}(r, \theta_3) &= u_{2r}(r, \theta_3) \\ u_{3\theta}(r, \theta_3) &= u_{2\theta}(r, \theta_3) \end{aligned} \quad (8)$$

For the same reason, we also have to consider the continuous variation of the shear and hoop stress components across the interface. Additional four constraints are thus imposed on the problem:

$$\begin{aligned} \sigma_{1\theta\theta}(r, \theta_1) &= \sigma_{2\theta\theta}(r, \theta_1) \\ \sigma_{1r\theta}(r, \theta_1) &= \sigma_{2r\theta}(r, \theta_1) \\ \sigma_{3\theta\theta}(r, \theta_3) &= \sigma_{2\theta\theta}(r, \theta_3) \\ \sigma_{3r\theta}(r, \theta_3) &= \sigma_{2r\theta}(r, \theta_3) \end{aligned} \quad (9)$$

It is clear that the system of constraints $[A(\lambda)]_{12 \times 12} \{x\} = \{0\}$, where $[A(\lambda)]$ is the matrix of the system, is underdetermined and cannot be solved directly. The nontrivial solution of this system requires that

$$\det [A(\lambda)] = 0 \quad , \quad (10)$$

from which the eigenvalues λ can be obtained. However, it is necessary to note that the analytical expression of the determinant is complex and therefore the only feasible way is to solve the system numerically.

The remaining twelve unknown constants a_i, b_i, c_i, d_i for $i = 1, 2, 3$ depend on particular eigenvalue λ . However, the solution should be performed carefully, because the only proportions of eleven constants to the twelfth one can be obtained due to nonuniqueness of the

solution. In the literature, one row of the mentioned system of the algebraic equations is usually eliminated and the column corresponding to the chosen constant moves into the right-hand side of the system with the opposite sign. This procedure can sometimes yield coefficients that correspond to very small values of the associated amplitude of the stress field. Neglecting these values that are related to fracture-mechanical parameters can erroneously predict the onset of crack propagation. Conditions of uniqueness of the fracture-mechanical parameters are discussed in the Dissertation.

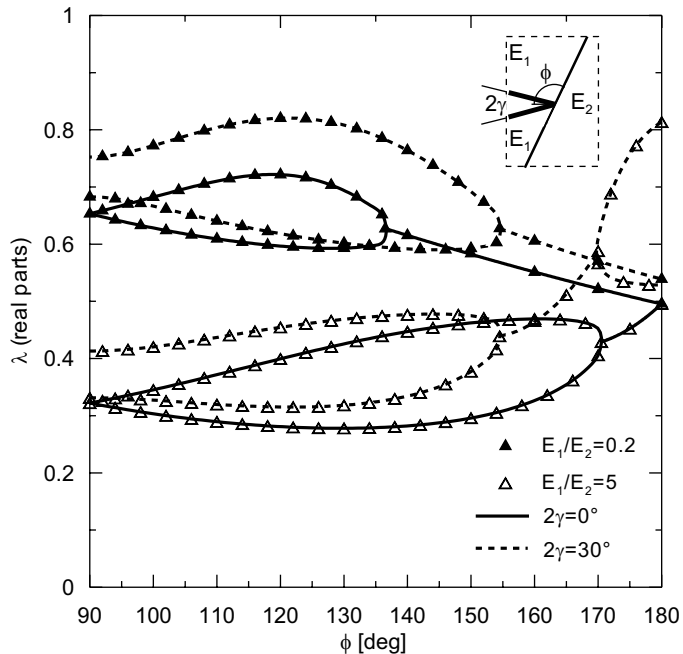


Figure 2: Variation of the real parts of eigenvalues λ with the angle ϕ for notch. Two distinct configurations, namely crack (solid line) and 30° notch (dotted line) are shown in the figure. Both materials have the same Poisson's ratio $\nu_1 = \nu_2 = 0.3$. Plane stress condition used.

Once the coefficients a_i, b_i, c_i, d_i are determined, the only unknown constants are A_k introduced in (2). As was mentioned above, these parameters cannot be quantified directly from the analytical approach, because they depend on loading, geometry, and boundary conditions usually applied far away from the notch faces. Instead, a modeling of the specimen with the prescribed boundary conditions has to be used to quantify these parameters.

4.2 Fracture-mechanical parameters and their physical meaning

We already know that the limited number of coefficients A_k is needed to fully describe the stress state of the cracked body. The amount of these coefficients equals to the number of eigenvalues λ_k taken for the description of the stress state. For example, a notch with nonzero angle 2γ perpendicular to the interface has three essential eigenvalues, two of them $0 < (\lambda_1, \lambda_2) < 1$ defining the singular stress terms and the last one corresponding to $\lambda_3 = 1$ with a regular stress distribution around the notch tip.

For eigenvalues in the region $0 < \lambda_k < 1$ we define the generalized stress intensity factor H_k such that $A_k = H_k/\sqrt{2\pi}$. On the other hand, eigenvalue $\lambda_3 = 1$ refers to the nonsingular term

of the Williams eigenfunction expansion (2). The coefficient A_3 is expressed as the so-called T-stress given by $A_3 = T/4$.

In homogeneous material, the T-stress is directly equal to the radial stress component along the crack faces or equivalently to the difference $\sigma_{rr} - \sigma_{\theta\theta}$ ahead of the crack tip, i.e. for $\theta = 0$. Physically, the T-stress is often regarded as a measure of the so-called *constraint* or triaxiality of stresses ahead of the crack tip [10].

Under the proposed assumptions, the Williams' solution (2) in the neighborhood of the V-notch tip can be written in terms of the fracture-mechanical parameters as

$$\Phi_i = \sum_{k=1}^{\max.2} \frac{H_k}{\sqrt{2\pi}} r^{\lambda_k+1} F_{ik}(\theta, \lambda_k) + \frac{T}{4} r^2 F_{i3}(\theta, 1) \quad . \quad (11)$$

Expressing the polar stress components related to the stress function Φ_i , one can obtain the following set of equations defining the polar stress field around the notch tip in terms of the chosen fracture-mechanical parameters:

$$\begin{aligned} \sigma_{iab} &= \sum_{k=1}^{\max.2} \frac{H_k}{\sqrt{2\pi}} r^{\lambda_k-1} f_{iab}^{(k)}(\theta, \lambda_k) + \frac{T}{4} f_{iab}^{(3)}(\theta, 1) \\ u_{ia} &= \sum_{k=1}^{\max.2} \frac{H_k}{\sqrt{2\pi}} r^{\lambda_k} g_{ia}^{(k)}(\theta, \lambda_k) + \frac{T}{4} r g_{ia}^{(3)}(\theta, 1) \quad , \end{aligned} \quad (12)$$

where a, b correspond to polar coordinates r, θ . Note that the entire series (11) and (12) contain either two or three terms depending on the number of eigenvalues in $0 < \lambda_k < 1$.

Both the generalized stress intensity factors H_k and T-stress are to be quantified from the numerical analysis of the whole body subjected to applied loading and prescribed boundary conditions. It was discovered in the past that these parameters can serve as criteria of the crack/notch stability based on the assumptions of the linear-elastic fracture mechanics. For a crack in homogeneous body ($\gamma = 0$), the generalized stress intensity factor H merges with the usual stress intensity factor K . In this case, the crack instability occurs when K reaches its critical value K_C known as the *fracture toughness*.

The more recent works, however, showed that also T-stress has a significant influence on the crack stability and the two-parameter fracture mechanics based on both parameters K and T was introduced. According to this theory, the crack instability occurs when the crack state defined by these two factors falls into the so-called *fracture toughness locus*. In the two-parameter fracture mechanics, the fracture toughness is therefore not a material characteristic, but depends on the magnitude of T-stress as a measure of constraint ahead of the crack tip.

5 QUANTIFICATION OF THE FRACTURE-MECHANICAL PARAMETERS

5.1 Extrapolation of the GSIF and T-stress

The process of direct calculation of the GSIFs immediately follows from the expression of the stress field (5). The approximation can be done on the basis of any stress component; here we choose $\sigma_{\theta\theta}$, for instance. Writing the analytical expression of the hoop stress components under two different angles θ_1 and θ_2 and neglecting the effect of the T-stress, one can conveniently

write the two conditions for the calculation of the GSIFs in matrix form as

$$\begin{bmatrix} r^{\lambda_1-1}\lambda_1(\lambda_1+1)F_2^{(1)}(\theta_1, \lambda_1) & r^{\lambda_2-1}\lambda_2(\lambda_2+1)F_2^{(2)}(\theta_1, \lambda_2) \\ r^{\lambda_1-1}\lambda_1(\lambda_1+1)F_2^{(1)}(\theta_2, \lambda_1) & r^{\lambda_2-1}\lambda_2(\lambda_2+1)F_2^{(2)}(\theta_2, \lambda_2) \end{bmatrix} \begin{Bmatrix} H_1 \\ H_2 \end{Bmatrix} = \begin{Bmatrix} \sigma_{2\theta\theta}(\theta_1)\sqrt{2\pi} \\ \sigma_{2\theta\theta}(\theta_2)\sqrt{2\pi} \end{Bmatrix} \quad (13)$$

Numerically, we have a set of internal points aligned radially at angles θ_1 and θ_2 . The points lying in immediate neighborhood of the notch tip have to be excluded from our analysis, because the stress field ahead of the notch tip contains both the elastic and plastic parts. Similarly we should not also take into account the internal points far away from the notch tip that are influenced by the finiteness of the sample. The sought generalized stress intensity factors are then determined as the intercepts of the obtained regression lines, see Fig. 3.

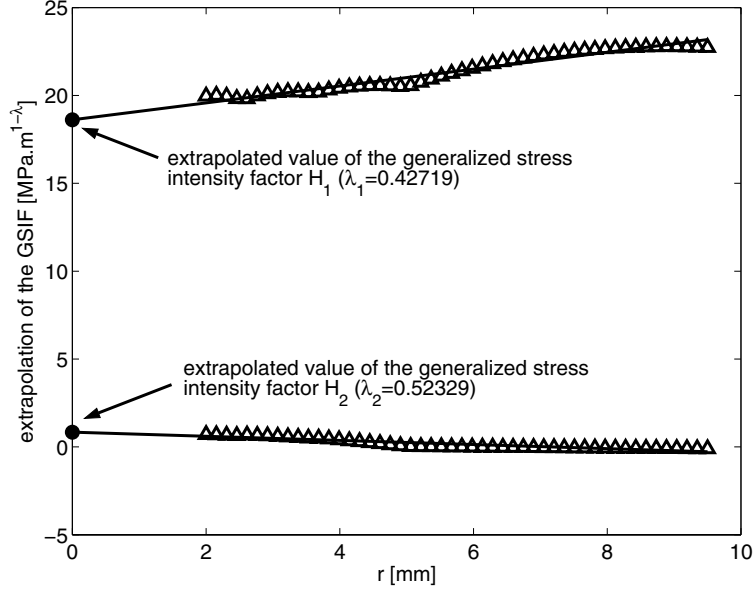


Figure 3: Extrapolation of the GSIF for a 30° notch, $E_1/E_2 = 2$, $\nu_1 = \nu_2 = 0.3$, $\phi = 105^\circ$, plane strain condition. The unknown magnitudes of the GSIF are equal to intercepts of the regression lines.

This method of quantification of the GSIF takes into account only the singular stress fields, whereas the rest of the Williams expansion is neglected. In contrast, the numerically obtained values of the stress components involve the whole Williams series without any conceivable separation of one term from another. Since the two expressions are not fully compatible due to different number of terms taken into account, also the GSIFs are determined only approximately.

Similar method can also be used to determine the magnitude of the T-stress. Because of the significant influence of plastic stresses at the notch tip, we have to again exclude a few of the internal points lying very close to the notch tip. Due to the finiteness of our numerical model, the points very far from the tip are excluded accordingly. The T-stress can then be simply expressed by taking into account both the singular and nonsingular stress terms. One of the possible and the simplest schemes for evaluation of the T-stress is to express the stress difference $\sigma_{rr} - \sigma_{\theta\theta}$ along angle $\theta = 0^\circ$ resulting in

$$T = \frac{4}{F_2^{(3)''}} \lim_{r \rightarrow 0} \left\{ \sigma_{2rr} - \sigma_{2\theta\theta} - \sum_{k=1}^n \frac{H_k}{\sqrt{2\pi}} r^{\lambda_k-1} \left[F_2^{(k)''} + (1 - \lambda_k^2) F_2^{(k)} \right] \right\}, \quad (14)$$

where $F_2^{(3)}$ is the eigenfunction corresponding to eigenvalue $\lambda_3 = 1$ calculated for domain 2 (see Fig. 1). Similarly, $F_2^{(k)}$ is the eigenfunction for eigenvalue λ_k valid for domain 2. Once the generalized stress intensity factors are determined, one can use (14) to obtain the variation of T with the radial distance. The approximated magnitude of the T-stress is then determined by extrapolating the regression line to $r = 0$.

5.2 Integral approach to the calculation of the GSIF

The reciprocal work contour integral method follows from the validity of the Betti reciprocal theorem. Since we have two independent configurations with the absence of body forces and assuming that they both satisfy the same boundary conditions, it is stated that:

The work of forces of the first system done on displacements of the second system equals to the work done by the forces of the second system on displacements of the first one.

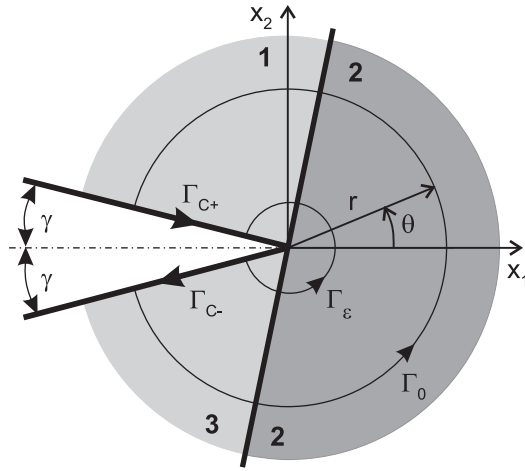


Figure 4: Contour paths for the calculation of the GSIFs

Let us have a closed contour Σ surrounding a V-notch tip defined by continuous segments Γ_{C-} , Γ_0 , Γ_{C+} , and Γ_ϵ such that $\Sigma = \Gamma_{C-} \cup \Gamma_0 \cup \Gamma_{C+} \cup (-\Gamma_\epsilon)$, as seen in Fig. 4. The reciprocal work theorem can then be written in integral form [14], [13] as

$$\oint_{\Sigma} (\sigma_{ij} u_i^* - \sigma_{ij}^* u_i) n_j ds = 0 \quad , \quad (15)$$

where n_j is positive unit outward normal of integration path Σ , σ_{ij} and u_i are components of the stress and displacement field, respectively, obtained from numerical analysis of the whole body with applied boundary conditions. In contrast, σ_{ij}^* and u_i^* are the stress and displacement components pertaining to analytical solution of the auxiliary problem that satisfies the same boundary conditions as the actual problem. For the time being, let us assume that this auxiliary solution corresponds to a specific eigenvalue $\lambda_l^* = -\lambda_l$. Hence, the stress and displacement field for the two states can be expressed as

$$\begin{aligned} \sigma_{ij} &= \sum_{k=1}^n A_k r^{\lambda_k - 1} f_{ij}(\lambda_k) & \sigma_{ij}^* &= A_l^* r^{-\lambda_l - 1} f_{ij}^*(-\lambda_l) \\ u_i &= \sum_{k=1}^n A_k r^{\lambda_k} g_i(\lambda_k) & u_i^* &= A_l^* r^{-\lambda_l} g_i^*(-\lambda_l) . \end{aligned} \quad (16)$$

Integrating (15) over a closed contour depicted in Fig. 4, one can easily see that the integration along the traction-free notch faces vanish. Hence, the integral identity between a near-tip field integration along Γ_ε and far field integration along Γ_0 is achieved:

$$\int_{\Gamma_0} (\sigma_{ij}u_i^* - \sigma_{ij}^*u_i)n_j ds = \lim_{\varepsilon \rightarrow 0} \int_{\Gamma_\varepsilon} (\sigma_{ij}u_i^* - \sigma_{ij}^*u_i)n_j ds \quad . \quad (17)$$

Since the stress field of both states is known analytically, it is possible to rewrite the near-tip field integration in the limit neighborhood of the notch tip as

$$\begin{aligned} \text{r.h.s.} &= \sum_{k=1}^n A_k A_l^* M_{kl} \lim_{\varepsilon \rightarrow 0} \varepsilon^{\lambda_k - \lambda_l} \\ M_{kl} &= \int_{-(\pi-\gamma)}^{\pi-\gamma} [f_{ij}(\lambda_k)g_i^*(-\lambda_l) - f_{ij}^*(-\lambda_l)g_i(\lambda_k)] n_j d\theta \end{aligned} \quad (18)$$

Here A_k is the unknown amplitude of the actual stress field, A_l^* is the amplitude of the auxiliary field and ε is the radial distance of contour Γ_ε . One can directly see, from the previous equation, that the interaction terms between the actual and auxiliary field vanish for $\lambda_k > \lambda_l$, where the corresponding component of the series vanishes in the limit neighborhood of the notch tip. When the eigenvalue of the auxiliary field λ_l^* is chosen to be a negative counterpart of λ_k , i.e. $\lambda_k = \lambda_l$, the corresponding term is of the form $A_k A_k^* M_{kk}$. The only interaction can thus follow from the terms, where $\lambda_k < \lambda_l$. Here, the right-hand side contains a diverging component. This nonphysical behavior can be removed only when M_{kl} is strictly orthogonal, i.e. when $M_{kl} \sim \delta_{kl}$ ¹.

Since the amplitude of the auxiliary field can be chosen arbitrarily, one can artfully define $A_k^* = 1/M_{kk}$. The unknown parameter A_k can then be evaluated as

$$A_k = \int_{\Gamma_0} (\sigma_{ij}u_i^* - \sigma_{ij}^*u_i)n_j ds \quad , \quad (19)$$

where all entries have been already explained above. This integration should be, in general case, carried out numerically, so that the accuracy of computation monotonously increases with increasing number of integration points. Furthermore, the notation (19) is symmetrical, which simplifies the integration process for symmetrical bodies. Consequently, the sought magnitude of the generalized stress intensity factor corresponding to a particular eigenvalue λ_k can be apparently obtained from the conventional relation $H_k = A_k \sqrt{2\pi}$.

Unfortunately, this algorithm could not be used equally well to determine the magnitude of the T-stress. This was so, because for every $\lambda = 1$, the M_{kk} integral was equal to zero and thus the corresponding magnitude of A_k^* was infinite. Since A_k^* is also used in the right-hand side of (19), this method is not useful for the quantification of the magnitude of T-stress.

5.3 On the calculation of T-stresses using the contour integrals

Although the J-integral is path-independent for cracks, where it measures the strain energy of the singular stress field, it is not equally well applicable to V-notches, where it lacks its

¹Orthogonality of M_{kl} has been proven numerically for a set of eigenvalues $0 < (\lambda_k, \lambda_l) \leq 1$. However, for greater eigenvalues λ_l the orthogonality is not attained strictly. This can cause serious problems in evaluating the amplitude of the corresponding actual field and thus the method requires an extensive mathematical analysis.

path-dependence. A generalization of the concept of contour integrals to V-notches led to the formulation of the so-called M-integral [7]:

$$M = \int_{\Sigma} (Wn_j - t_i u_{i,j}) x_j ds \quad (20)$$

Superimposing two independent linear-elastic solutions, one of them called the actual field (A) and the other being the auxiliary field (B), one can express the interaction M-integral between these two states as follows:

$$M^{(A,B)} = M^{(A+B)} - M^A - M^B \quad , \quad (21)$$

where $M^{(A+B)}$ is the superimposed M-integral and M^A, M^B denote the two M-integrals corresponding to actual and auxiliary field, respectively.

Substituting the expressions for the M-integral, rearranging, and realizing that the elastic moduli of both actual field and auxiliary field are identical, one obtains the fundamental formula for the quantification of the interaction M-integral:

$$M^{(A,B)} = \int_{\Gamma_0} \left(\sigma_{ik}^B \varepsilon_{ik}^A - \sigma_{ij}^A u_{i,j}^B - \sigma_{ij}^B u_{i,j}^A \right) n_j x_j ds \quad , \quad (22)$$

Note that the parameters corresponding to the actual field (A) are determined numerically, whereas the auxiliary solution has to be known analytically. This is clearly the major complication associated with such a method. So far, the auxiliary field has been derived only for a crack in homogeneous material and interface crack [15]. The auxiliary solution is often taken as the solution to a concentrated point force $\underline{f} = (f_1, f_2)$ applied at the crack tip.

To make the methodology valid for an arbitrarily oriented V-notch terminating at a bimaterial interface, the two states (A) and (B) have to satisfy the same boundary conditions along the notch faces and also along the interface between the two layers. Moreover, to maintain the path-independence of the mutual M-integral, also the partial derivatives of the displacement components must be continuous in both states A, B along the interface between domain a and b , i.e.:

$$u_{i,j}^{A|a} = u_{i,j}^{A|b} \quad \wedge \quad u_{i,j}^{B|a} = u_{i,j}^{B|b} \quad . \quad (23)$$

Unfortunately, this cannot be generally achieved, as is proved in the Dissertation.

Consequently, an attempt to exceed this type of calculation to a general case of a V-notch terminating at the interface between two elastic materials was not successful. To quantify the magnitude of T-stress for further considerations about its importance, one has to use the extrapolation technique briefly discussed in the previous chapter.

5.4 Assessment of the stability of bimaterial V-notches

One of the most logical and computationally feasible ways of the assessment of the stability of cracks and notches is to make use of the Sih's criterion of the strain energy density. According to this criterion, the further crack propagation is assumed in a direction of minimum strain energy density. Since we use the well-known expression for the energy density of a small volumetric element and express the stress tensor using its components, we immediately obtain the fundamental expression of the strain energy density

$$\frac{\Sigma}{r} = \frac{dW}{dV} = \frac{1}{4\mu} \left[\frac{\kappa + 1}{4} (\sigma_{rr} + \sigma_{\theta\theta})^2 - 2(\sigma_{rr}\sigma_{\theta\theta} - \sigma_{r\theta}^2) \right] \quad , \quad (24)$$

where Σ is the generalized strain energy density factor, μ is shear modulus of the target material (uncracked material towards which the crack is going to propagate), $\kappa = 3 - 4\nu$ for plane strain and $\kappa = (3 - \nu)/(1 + \nu)$ for plane stress is the elastic constant of the target material and σ_{ij} are components of the stress tensor field.

Now let us take into account all the singular stress terms corresponding to $0 < \lambda < 1$ and also the nonsingular term derived for $\lambda = 1$. Substitution of the polar stress components (5) into (24) then yields a more appropriate expression of the generalized strain energy density factor Σ :

$$\Sigma = A_{11}H_1^2 + 2A_{12}H_1H_2 + A_{22}H_2^2 + A_{13}H_1T + A_{23}H_2T + A_{33}T^2, \quad (25)$$

where H_1, H_2 are the generalized stress intensity factors corresponding to the particular eigenvalues λ_1, λ_2 and T is the T-stress corresponding to eigenvalue $\lambda = 1$. The remaining coefficients A_{ij} can be easily derived and are written in expanded form in the Dissertation.

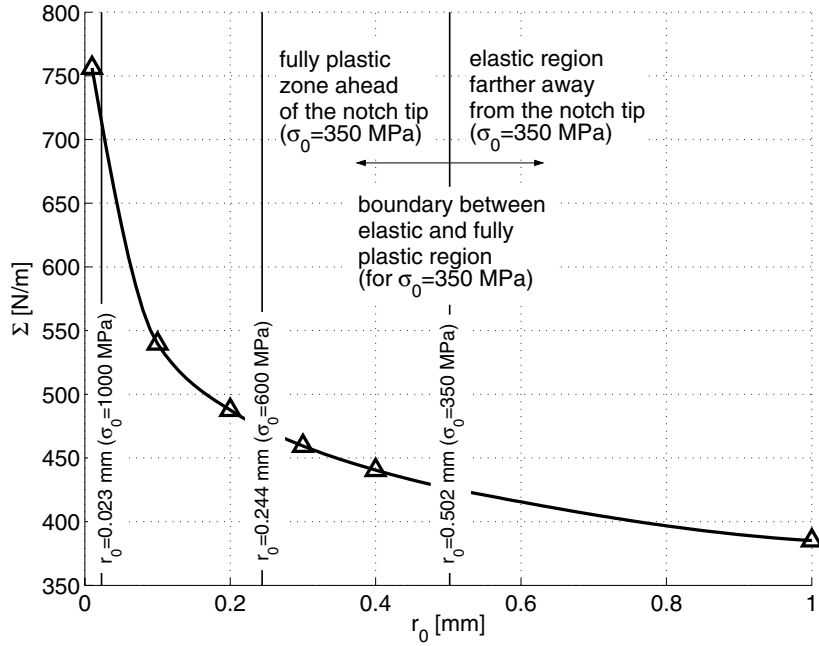


Figure 5: Variation of the modified Sih's strain energy density factor Σ with different choices of the radial distance r_0 at which it is evaluated. These results were obtained for a 30° notch perpendicular to the interface, $E_1/E_2 = 2$, $\nu_1 = \nu_2 = 0.3$, yield stress $\sigma_0 = 350$ MPa, plane strain condition used.

From the condition that the crack propagation occurs in the direction of minimum strain energy density, one can easily obtain the initial crack propagation direction θ_0 by minimizing the generalized strain energy density factor:

$$\left(\frac{\partial \Sigma}{\partial \theta} \right)_{\theta=\theta_0} = 0, \quad \left(\frac{\partial^2 \Sigma}{\partial \theta^2} \right)_{\theta=\theta_0} > 0. \quad (26)$$

Note, that this minimization has to be carried out at a certain radial distance r_0 centered at the notch tip. Choice of such a value is crucial in determining the factor Σ . According to Knésl [9] and Náhlík [12], this parameter can be conveniently chosen such that it reflects some physical property like the radius of the plastic region, average grain size, etc. However,

different choices of the radius r_0 can yield very different magnitudes of the Sih's factor Σ , as seen for a particular notch configuration in Fig. 5.

Now, define a critical value of the generalized strain energy density factor Σ_C as a value corresponding to a state in which an unstable crack propagation, i.e. brittle failure, occurs. Following the modification of the usual Sih's strain energy density criterion, we can now state that the propagation of a microcrack at the tip of the V-shaped notch towards the target layer will not occur if the following stability criterion is satisfied:

$$\Sigma(r_0, \theta_0) < \Sigma_C \quad (\text{stability}) . \quad (27)$$

It is rather trivial to prove that the dimension of Σ is now independent of the geometrical properties of notch and also of the "strength" of its singularity. Consequently, the critical value Σ_C can be regarded as a material characteristic and Eq. (27) provides us with an unambiguous condition for the assessment of stability of our general stress concentrators.

6 INTRODUCTION TO THE BOUNDARY ELEMENT METHOD

6.1 Governing equation of elastostatics

Boundary Element Method (BEM) as a computational tool for an exact description of real behavior of the modeled bodies is based on the validity of the Betti reciprocal work theorem between two independent states of equilibria. One of the main features of BEM is the necessary knowledge of the fundamental solution of the given problem.

It is known from the theory of elasticity that the system at equilibrium has to satisfy the so-called Cauchy relations. Assume the theory of small deformations that requires a sufficiently small deflections, so that the higher order terms of the strain tensor can be neglected comparing to the leading term. The Cauchy relations can then be written in terms of the displacement derivatives as

$$\mu u_{i,kk} + (\lambda + \mu) u_{k,ki} + X_i = 0 \quad , \quad (28)$$

where μ is the shear modulus and $\lambda = E\nu/[(1 + \nu)(1 - 2\nu)]$ is the Lamé constant.

Equation (28) is the governing partial differential equation of the two dimensional linear-elastic problems, which are of interest in this Dissertation. For the use in the Betti reciprocal work theorem, we define two independent elastic configurations. One of the systems involved in the method will be our numerical model with the boundary conditions that are now prescribed only on the boundary. The second system corresponds to an infinite plane with the fundamental solution obtained as a real space solution of the following partial differential equation:

$$\mu U_{ik,jj} + (\lambda + \mu) U_{jk,ji} = -\delta_{ik} \delta(\underline{x} - \underline{y}) \quad , \quad (29)$$

where $U_{ik}(\underline{x}, \underline{y})$ can be understood as the i -th component of the displacement at point \underline{x} of an infinite plane in response to a concentrated force on the body, acting in the k -th direction at point \underline{y} , i.e. $X_l(\underline{x}) = \delta_{kl} \delta(\underline{x} - \underline{y})$.

Applying the Fourier transform, the equation (29) can be converted into a system of algebraic equations, from which we can directly express the Fourier images $\bar{U}_{ik}(\underline{k})$. Now, performing the inverse Fourier transform one obtains the fundamental displacements as solutions of (29) in the real space called the *Kelvin solutions*. The corresponding fundamental traction

on the boundary of the model can be expressed from the relationship between traction and stress components. Finally, the Kelvin solutions are as follows:

$$\begin{aligned} U_{ik}(\underline{x}, \underline{y}) &= \frac{1}{8\pi\mu(1-\bar{\nu})} [-(3-4\bar{\nu})\delta_{ik} \ln r + r_{,i}r_{,k}] \\ T_{ik}(\underline{x}, \underline{y}) &= \frac{1-2\bar{\nu}}{4\pi(1-\bar{\nu})r} \left[r_{,k}n_i(\underline{x}) - r_{,i}n_k(\underline{x}) - \left(\delta_{ik} + \frac{2}{1-2\bar{\nu}}r_{,i}r_{,k} \right) r_{,j}n_j(\underline{x}) \right] \quad , \quad (30) \end{aligned}$$

where the points \underline{x} , \underline{y} introduced above are separated by $r = |\underline{x} - \underline{y}|$, further $r_{,i}$ is the partial derivative of r with respect to the i -th Cartesian component and c_{ijml} is the elastic stiffness tensor. Note that both the Kelvin solutions U_{ik} and T_{ik} are singular with respect to the distance r .

Applying the Betti reciprocal theorem onto these two systems, we can derive the basic relation between the forces and displacements of both systems in the form of the well-known *Somigliana identity*:

$$u_k(\underline{y}) = \int_S \left[t_i(\underline{x})U_{ik}(\underline{x}, \underline{y}) - u_i(\underline{x})T_{ik}(\underline{x}, \underline{y}) \right] dS_x \quad , \quad (31)$$

where \underline{y} is an internal point, $u_i(\underline{x})$ and $t_i(\underline{x})$ are boundary displacements and tractions and the tensorial components $U_{ik}(\underline{x}, \underline{y})$, $T_{ik}(\underline{x}, \underline{y})$ were defined in Eq. (30). The integration has to be carried out along the entire boundary \bar{S} . Note that the equation (31) is valid only for internal points. Moving the internal point \underline{y} onto the boundary, the Somigliana identity transforms to a constraint equation and the integral containing T_{ik} must be performed in the CPV-sense.

In the subsequent text, we will use a designation *hypersingular* when referring to a term proportional to r^{-2} , *strongly singular* for the terms proportional to r^{-1} and *weakly singular* for the singularities of the type $\ln r$, as suggested by Mukherjee [11].

6.2 Calculation of internal displacements

The strongly singular representation of internal displacements (31) gives a reasonable computational accuracy in the case when the internal point lies sufficiently far from the boundary. Consequently, the distance between the source point and field point is larger and the strong singularity of the kernel T_{ik} does not decay the accuracy of the regular Gaussian quadrature. However, when the internal point lies close to the boundary, or more accurately in the so-called *boundary layer*, the singularity of the kernel deteriorates the accuracy of calculation the more the closer the internal point is to the boundary². Apparently, the displacements at internal points lying inside this boundary layer cannot be assumed to be correct [16] and therefore a more appropriate scheme should be used.

One of the available methods that can be used to overcome the difficulty associated with the evaluation of the integral (31) introduces the effect of the boundary point $\underline{\zeta}$ that is closest to the internal point \underline{y} at which we determine the displacements. The point $\underline{\zeta}$ generally lies somewhere within a particular element and thus the displacement components $u_k(\underline{\zeta})$ can be approximated using the shape functions as usual.

²The thickness of the boundary layer depends on the strength of singularity, length of the element over which the integration is being performed and the number of Gauss points.

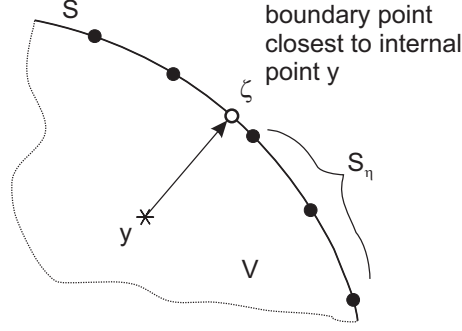


Figure 6: Selection of the nearest boundary point for the computation of displacements at internal point \underline{y} using the regularized integral formula (33).

Let us now subtract and add back to (31) the displacement of the nearest boundary point $\underline{\zeta}$, so that the integral equation modifies to

$$u_k(\underline{y}) = u_i(\underline{\zeta})\delta_{ik} + \int_S t_i(\underline{\eta})U_{ik}(\underline{\eta}, \underline{y}) dS_\eta - \left[\int_S u_i(\underline{\eta})T_{ik}(\underline{\eta}, \underline{y}) dS_\eta - u_i(\underline{\zeta}) \int_S T_{ik}(\underline{\eta}, \underline{y}) dS_\eta \right]. \quad (32)$$

Although this computational trick is rather straightforward, it should be noted that the last integral transforms to $-\delta_{ik}$ for the points sufficiently far from the boundary, i.e. essentially behind the boundary layer. In this case, however, the integral representation (32) simplifies back to the initial form (31). On the other hand, for the internal point \underline{y} located within the boundary layer, the equation (32) can be written more appropriately as

$$u_k(\underline{y}) = u_k(\underline{\zeta}) + \int_S t_i(\underline{\eta})U_{ik}(\underline{\eta}, \underline{y}) dS_\eta - \int_S [u_i(\underline{\eta}) - u_i(\underline{\zeta})] T_{ik}(\underline{\eta}, \underline{y}) dS_\eta. \quad (33)$$

This expression remains nonsingular for any internal point \underline{y} , even if this point lies on the boundary and is called the *regularized integral representation* of internal displacements.

To convince ourselves that the statement above is justified, let us assume the two points $\underline{\eta}, \underline{y}$, where $\underline{\eta}$ is a particular boundary node and \underline{y} lies generally anywhere around $\underline{\eta}$ including the case where the two points coincide. Require also that the boundary is sufficiently smooth at any boundary point or more precisely it is a *Lyapunov boundary* at any $\underline{\eta}$ [1]. Then the so-called *Hölder condition* must be satisfied in order to remove the singularity from the integral (33). Mathematically this condition is written as

$$|u(\underline{\eta}) - u(\underline{y})| \leq A|\underline{\eta} - \underline{y}|^\alpha, \quad (34)$$

where $0 < A < \infty$ and $0 < \alpha \leq 1$ determine the smoothness of the boundary. The elements in BEM are regarded as C^α continuous, where α is usually zero. For these simpler elements the continuity of shape functions is preserved, but the first derivatives are already discontinuous at the junction of the two neighboring elements. Several attempts have been made to use the more elaborate C^1 elements, but because of the tremendous mathematical difficulty of the underlying mathematics, the vast majority of them were not widely adopted by engineers.

6.3 Integral representation of internal stresses

According to the Hooke's law, the stress is proportional to the first derivative of displacements via the fourth-order tensor of elastic constants. From the Somigliana identity (31) we already

know that the displacements of any particular internal point \underline{y} in the BEM are determined on the basis of knowledge of the Kelvin solution U_{ik}, T_{ik} (30) obtained by solving the fundamental equation of elastostatics. Differentiating the displacement components (31) with respect to a general coordinate x_l and substituting them into the Hooke's law via the expressions for strains, one can see that the stress tensor at the particular internal point \underline{y} can be expressed as

$$\sigma_{kl}(\underline{y}) = \int_S [t_i(\underline{\eta})D_{kli}(\underline{\eta}, \underline{y}) - u_i(\underline{\eta})S_{kli}(\underline{\eta}, \underline{y})] dS_\eta \quad . \quad (35)$$

This is the so-called *hypersingular boundary integral representation of internal stresses*, because the integral kernel S_{kli} is hypersingular with respect to the distance between $\underline{\eta}$ and \underline{y} . Particular expressions for both D_{kli} and S_{kli} are given in [1] and reviewed also in this Dissertation.

If the distance between the internal point and the nearest boundary point is sufficient, the accuracy of calculation is good and the hypersingular stress representation (35) can be reasonably used. In contrast, if this distance is less than a half of the smallest boundary element [2], the accuracy of the calculation again fails very quickly within this boundary layer. In comparison to the nonregularized calculation of the internal displacements (31), the hypersingular kernel S_{kli} causes the accuracy to decay much faster and also the boundary layer zone is wider in this case.

The hypersingularity present in the kernel S_{kli} can be weakened by integrating the term associated with S_{kli} in (35) by parts. The hypersingular kernel thus transforms to a strongly singular tensorial operator \hat{T}_{kli} . Particular expression of this operator is again given in [1] and also discussed in this Dissertation. The hypersingular integral representation of the internal stresses (35) can be more conveniently written in the partly regularized strongly singular form

$$\sigma_{kl}(\underline{y}) = \int_S [t_i(\underline{\eta})D_{kli}(\underline{\eta}, \underline{y}) + \hat{T}_{kli}(\underline{\eta}, \underline{y})u_i(\underline{\eta})] dS_\eta \quad , \quad (36)$$

where \hat{T}_{kli} is the introduced tensorial operator. This approach yields a much narrower boundary layer, so that more accurate computation of stresses at internal points closer to the boundary can be achieved.

6.4 Numerical treatment at corner points

In the case where the model contains internal corners, a special care must be devoted to the treatment at the nodes associated with these corners. One of the most mechanically consistent procedures was recently published by Beer [2].

Assume that the model consists of three elastic domains with isotropic behavior. Since these domains are welded together, the internal interface is defined by three joints, namely horizontal interface I-II and two vertical interfaces I-III, II-III, where the numbers denote the two domains in contact - see Fig. 7. By "welding" we will mean the continuity of displacements and equilibrium of tractions along the interface. The following set of constraints is thus required:

$$\begin{aligned} u_k^I - u_k^{II} = 0 & \quad , & u_k^I - u_k^{III} = 0 & \quad , & u_k^{II} - u_k^{III} = 0 \\ t_k^I + t_k^{II} = 0 & \quad , & t_k^I + t_k^{III} = 0 & \quad , & t_k^{II} + t_k^{III} = 0 \quad , \end{aligned} \quad (37)$$

where u_k^α is a displacement component along the x_k axis on the boundary of domain α . Apparently, for n interface nodes, we now have $2(n+2)$ conditions, but only $2n$ tractions at

these points are unknown. The system of equations is therefore overdetermined and cannot be solved without additional treatment. An elegant way of overcoming this problem is to work with *equivalent nodal forces*, as proposed by Beer [2]. These forces are computed using the principle of virtual work step by step in all directions k .

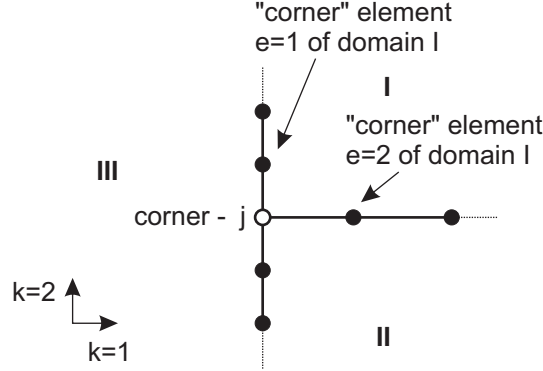


Figure 7: An internal corner formed at a joint of three domains.

Once we apply a virtual displacement $\delta u_k = 1$ at a corner point, the work done by tractions must be equal to that done by the equivalent nodal forces, i.e. the following identity is ensured:

$$F_k \cdot 1 = \int_S t_k \delta u_k \, dS \quad , \quad (38)$$

where F_k is the equivalent nodal force, t_k and δu_k are traction component and small displacement in the direction x_k , respectively. The integration is carried out over the two common elements connected to the corner. The traction force for any point along a particular element e and the virtual displacement can be further expressed as

$$t_k^e = \sum_{a=1}^n N_a t_k^{ae} \quad , \quad \delta u_k = N_j^e \delta u_k = N_j^e \cdot 1 \quad , \quad (39)$$

where N_j^e is the shape function of the corner in local (element) numbering and e counts the two elements that contain the corner j as their edge node. The equivalent nodal force corresponding to the virtual shift δu_k is then given by substituting Eq. (39) into (38):

$$F_k = \sum_{e=1}^2 \int_{S_e} N_j^e \sum_{a=1}^n N_a t_k^{ae} \, dS_e \quad . \quad (40)$$

We further assume that the virtual forces are in equilibrium at each corner node. Consequently, instead of writing the six equilibrium conditions for tractions (37) in 2-D, we require only the equilibrium of the virtual forces given as

$$F_k^I + F_k^{II} + F_k^{III} = 0 \quad . \quad (41)$$

By using the concept of virtual forces, we decreased the number of additional equations from six to two, i.e. we impose four less constraints for each corner node. Finally, for those n interface nodes quoted above, we now have $2n$ equations for $2n$ unknown tractions, where two traction conditions follow from each two coinciding nodes on the smooth part of the interface and two equilibrium constraints (41) are prescribed at each corner point in 2-D.

radius $R = 5$ mm centered at the notch tip. Simpson's method was used for the numerical evaluation of the contour integrals.

Consider now a V-notch with angle $2\gamma > 0^\circ$ and analyze the stress field in more detail. From the solution of the eigenvalue problem, we can clearly see that in this case we have two different eigenvalues in the region $0 < \lambda < 1$ and thus also two, generally different, values of the generalized stress intensity factors H . It can be easily proved that stress field is mainly affected by stronger singularities. Since the power of the singularity is expressed as $p = 1 - \lambda$, the major contribution is done by the stress terms involving the larger stress singularity exponent p or smaller eigenvalue λ .

Separating the cosine and sine terms of (4), one can define the opening stress intensity factor K_I corresponding to symmetric fields and in-plane shear stress intensity factor K_{II} corresponding to the antisymmetric fields. These two components can be calculated directly from the displacements in the vicinity of the crack tip, for example using the ANSYS command KCALC. However, it should be pointed out that the accuracy of such a calculation strongly depends on the smoothness of the mesh and also on the size of the notch tip element whose nodal displacements are used for the approximation of K_I and K_{II} . The magnitudes of the SIFs obtained from the finite element model of a crack embedded in a homogeneous domain were, in our case:

$$\begin{aligned} \phi = 90^\circ : & \quad K_I = 28.59 \text{ MPa.m}^{1/2} \quad , \quad K_{II} = 0 \text{ MPa.m}^{1/2} \\ \phi = 120^\circ : & \quad K_I = 25.27 \text{ MPa.m}^{1/2} \quad , \quad K_{II} = 8.10 \text{ MPa.m}^{1/2} \quad , \end{aligned}$$

where ϕ is the angle between the direction of loading and the crack.

Because the only generalized stress intensity factor pertaining to the smaller eigenvalue was calculated in the earlier work [8], the rest of the eigenvalues following from the solution of the eigenvalue problem are neglected at this point.

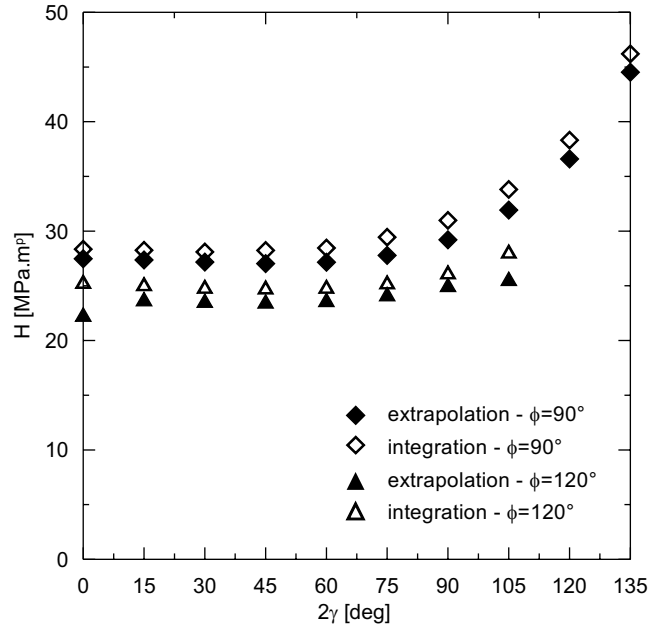


Figure 9: Comparison of the magnitudes of the generalized stress intensity factor H calculated using the direct method (13) in [8] and from the contour integral method.

The constant d_2 appearing in the eigenfunction (4) was taken as unity for further relevant comparison with the stress intensity factors obtained from the separation of the symmetric and antisymmetric parts of the solution published in [8]. As can be seen in Fig. 9, the SIFs determined using ANSYS are in good agreement with the contour integral method. Similarly, comparison of the direct and contour integral approach shows a rather promising agreement of both methods.

As seen in Fig. 9, the relative comparison of the direct and integral method reasonably correspond to each other with the maximum relative error of approximately 12 % for crack ($2\gamma = 0^\circ$). In this case, the stress distribution in the vicinity of the notch tip is rather uniform and also displacements at the internal points around the notch tip vary gradually without steep gradients. It is therefore not surprising that both the direct method and contour integral method yield very close results.

At this point, we cannot draw any conclusion about the stability of the notch, because the dimension of the GSIF depends on the geometry of the notch. This is rather unfortunate in the sense that for each notch opening, we would need to have a special critical value, somewhat like generalized fracture toughness³. Clearly the only reasonable comparison between the actual stress state given by the set of calculated GSIFs and the critical stress state is possible by application of a suitable fracture-mechanical criterion.

7.2 A notch perpendicular to bimaterial interface

Let us assume that the crack had initiated at a surface scratch or microcrack left by the fabrication or machining process. Under the external loading, the sharp tip of this flaw behaves as a source of elevated stresses that lead in brittle materials to enhanced microcracking and further formation of a dominant crack. In the layered materials with homogeneous microstructure of both layers, the crack grows preferentially in the direction perpendicular to the maximum applied stress. After approaching the interface the crack can either debond the two layers or penetrate into the the target layer. Under certain circumstances, mainly when the target layer is ductile, a significant blunting of the crack tip can result in the crack arrest, as was discussed by De Hosson [4] on the basis of experimental observations.

Here we are particularly interested in the situation, where the microcrack emanating from a larger bimaterial crack or notch penetrates the interface and propagates towards the target layer. Full numerical model was again used to be consistent with further results obtained for an inclined crack terminating at the interface. The geometry of the specimen was defined by the widths of the two layers $W_1 = 12$ mm, $W_2 = 38$ mm and full length $L = 250$ mm. Various Young's moduli of both materials were used to model the distinctive levels of inhomogeneity of the interface, Poisson's ratio $\nu_1 = \nu_2 = 0.3$ was constant for both materials. Plane strain case was used as in the previous analysis.

The vector of coefficients $\{x\}$ in eigenfunction (4) was always chosen such that the coefficients merged with the standard values for a crack in homogeneous material. This was achieved

³The term generalized fracture toughness is not widely accepted. The reason for this is hidden in the physical character of the problem, where for any geometry of a V-notch embedded in a homogeneous linearly-elastic material, we would need to measure the critical value of the GSIF. This is even more apparent if we remember that for a general V-notch, two generalized stress intensity factors are present. Obviously, the experiments that would be needed to investigate the variation of this hypothetical generalized fracture toughness would be rather complex.

by dividing the vector corresponding to the lesser of the two eigenvalues by d_2 . However, this adjustment cannot be done for the remaining greater eigenvalue, where d_2 is close to zero. Instead, in all these cases the coefficient vector $\{x\}$ was normalized. Since the same vector of coefficients is always used together with the generalized stress intensity factor calculated from it, there is no inconvenience associated with the different approach to the choice of the coefficient vector.

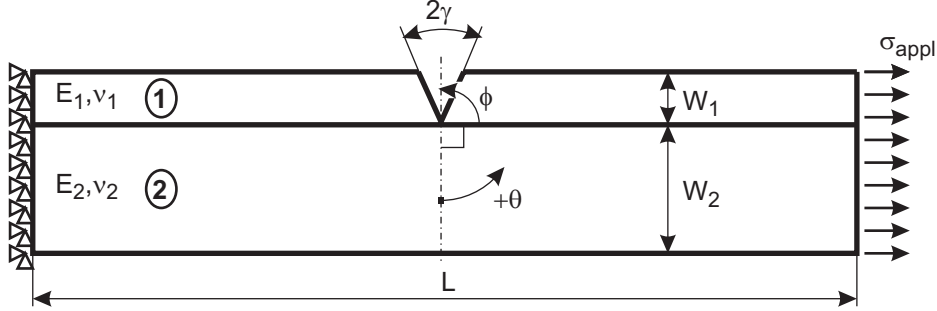


Figure 10: Model of a bimaterial V-notch normal to the interface between two elastic layers.

The direct calculation of the generalized stress intensity factors (13) was carried out using the extrapolation along two different angles ahead of the notch tip, namely $\theta_1 = -5^\circ$, $\theta_2 = 5^\circ$, where zero corresponds to the direction towards the ligament. The character of the external loading in this case causes a domination of one of the generalized stress intensity factors over the second one. The T-stresses for these nonhomogeneous interfaces were calculated purely using the direct extrapolation technique. Because the contour integral method is applicable only for the integration paths not crossing the nonhomogeneous interface, the relevant comparison with the direct method can be made only between the homogeneous cases.

It should be also pointed out that we cannot generally assign any physical meaning to any of the values H from the reasons that were explained at the end of the preceding chapter. Since the physical interpretation of the elastic T-stresses for general bimaterial V-notches has not been given yet, we should regard the T-stress, for the time being, only as an amplitude of the nonsingular stress field. This is a clear difference from the classical fracture-mechanical theory of cracks in homogeneous bodies, where the T-stress is a measure of the triaxiality of stresses ahead of the crack tip. Consequently, the only relevant comparison between the actual state of the body and the critical state corresponding to the onset of unstable crack propagation and delamination of the specimen can be made on the indirect basis.

Calculation of Σ at $r_0 = 0.01$ mm

To reveal the influence of parameter r_0 on the magnitude of the modified Sih's strain energy density factor Σ , we first choose $r_0 = 0.01$ mm without any physical justification of this choice. The obtained values of the factor Σ are summarized in Tab. 1. One can see that Σ significantly varies with the mismatch of elastic properties of the bonded layers. In the case when the V-notch lies in softer material and further propagation into the stiffer substrate is assumed ($E_1/E_2 < 1$), the Σ factor is small in comparison to the case when the defect propagates from stiff material to the more compliant one ($E_1/E_2 > 1$).

From the obtained table we can also conclude that the magnitudes of the modified Sih's strain energy density factor Σ calculated using both singular and nonsingular stress terms, i.e. accounting the GSIFs and T stress, only slightly differ from the values calculated purely from the GSIFs. This means that the primary role in the assessment of the stability of bimaterial V-notches play the singular stress fields, whereas the stress terms nonsingular with respect to the radial distance can be regarded as unnecessary corrections in this particular case.

Sih's modified strain energy density factor Σ calculated at $r_0 = 0.01$ mm						
E_1/E_2	$2\gamma = 0^\circ$		$2\gamma = 30^\circ$		$2\gamma = 60^\circ$	
	$\Sigma(H)$	$\Sigma(H, T)$	$\Sigma(H_1, H_2)$	$\Sigma(H_1, H_2, T)$	$\Sigma(H_1, H_2)$	$\Sigma(H_1, H_2, T)$
0.5	56.81	59.08	54.35	55.16	45.85	46.80
0.6	128.32	130.51	114.74	115.17	95.58	96.63
1.0	328.14	323.22	315.59	314.63	267.63	268.46
1.5	488.67	484.73	541.06	538.89	480.73	480.70
2.0	617.03	615.29	756.20	753.98	699.77	699.32

Table 1: Magnitudes of the generalized strain energy density factor Σ for a notch perpendicular to the interface ($\phi = 90^\circ$) calculated purely from the GSIFs and also accounting for both GSIF and T-stress. Dimensions: Σ [N/m]

Moreover, one can observe that for certain configurations highlighted in Tab. 1, the Σ factor for notch is higher than the corresponding value for a crack. Note that this discrepancy is associated only with the configurations of a notch that propagates from a stiff coating into a more compliant elastic material of substrate. In this case the plastic region ahead of the notch tip is significantly larger in comparison to the homogeneous case. Namely, radius of the plastic region ahead of the notch tip was approximately 0.42 – 0.46 mm for $E_1/E_2 = 1.5$ and 0.50 – 0.53 mm for $E_1/E_2 = 2$. For comparison, the radius of the plastic region in homogeneous body was approx. 0.28 – 0.35 mm and between 0.03 – 0.09 when $E_1/E_2 = 0.5$.

Since the plastic region is significantly larger for $E_1 > E_2$, one of the reasonable justifications of this discrepancy could be a possible breakdown of the linear elasticity, which requires the plastic zone to be negligible in comparison to the size of the model. If the linear elasticity is used, in spite of this fact, the results imply that in the current model there is a certain critical angle of notch for which the factor Σ reaches a maximum value. From practical point of view, this would apparently mean that for a notch perpendicular to the interface between two elastic materials, where the coating is stiffer than substrate ($E_1/E_2 > 1$), the critical configuration is not associated strictly with the sharp crack, but depends on the mismatch of the elastic properties of both layers.

Calculation of Σ and θ_0 at the plastic zone boundary

To learn more about the influence of r_0 on the corresponding magnitudes of Σ and the crack propagation direction θ_0 , we carried out another analysis with a more convenient choice of r_0 . Here we choose r_0 such that it will be equal to the radius of the plastic zone ahead of the notch tip in the direction given by the notch axis. The yield stress was chosen as $\sigma_0 = 350$ MPa, for which the corresponding radii r_0 are of measurable magnitude. Dependence $\Sigma(r_0)$ for different yield stresses was already introduced for a particular configuration in Fig. 5.

The most important information included in Tab. 2 is again written in bold. Let us now turn our attention to the first column containing the data obtained for a sharp crack ($2\gamma = 0^\circ$).

One can observe that with increasing ratio E_1/E_2 , i.e. the material of substrate becomes increasingly more compliant in comparison to the material of coating, the factor Σ monotonously increases up to its maximum corresponding to $E_1/E_2 = 1.5$ and then it surprisingly falls below this value. There is of course no physical reason for this decay.

Sih's modified strain energy density factor Σ calculated at the plastic zone boundary						
E_1/E_2	$2\gamma = 0^\circ$		$2\gamma = 30^\circ$		$2\gamma = 60^\circ$	
	$\Sigma(H)$	$\Sigma(H, T)$	$\Sigma(H_1, H_2)$	$\Sigma(H_1, H_2, T)$	$\Sigma(H_1, H_2)$	$\Sigma(H_1, H_2, T)$
	$\theta_0(H)$	$\theta_0(H, T)$	$\theta_0(H_1, H_2)$	$\theta_0(H_1, H_2, T)$	$\theta_0(H_1, H_2)$	$\theta_0(H_1, H_2, T)$
	$r_0 = 0.026$		$r_0 = 0.048$		$r_0 = 0.090$	
0.5	75.03	73.40	69.20	71.30	72.41	76.07
	<i>+18.73</i>	<i>+16.66</i>	<i>+0.55</i>	<i>+0.49</i>	<i>-0.04</i>	<i>-0.04</i>
	$r_0 = 0.127$		$r_0 = 0.154$		$r_0 = 0.209$	
0.6	163.02	154.39	147.46	149.79	142.46	148.49
	<i>+12.92</i>	<i>+10.61</i>	<i>+0.44</i>	<i>+0.37</i>	<i>-0.05</i>	<i>-0.05</i>
	$r_0 = 0.286$		$r_0 = 0.304$		$r_0 = 0.354$	
1.0	328.14	304.06	318.74	314.46	292.00	297.96
	<i>0.00</i>	<i>+3.84</i>	<i>-0.02</i>	<i>-2.25</i>	<i>-0.01</i>	<i>-2.64</i>
	$r_0 = 0.421$		$r_0 = 0.429$		$r_0 = 0.466$	
1.5	354.81	333.67	392.90	381.36	357.44	357.42
	<i>-14.23</i>	<i>-12.70</i>	<i>-0.79</i>	<i>-0.67</i>	<i>+0.18</i>	<i>+0.16</i>
	$r_0 = 0.500$		$r_0 = 0.502$		$r_0 = 0.529$	
2.0	344.45	335.34	426.09	414.54	394.27	391.92
	<i>-21.67</i>	<i>-20.91</i>	<i>-1.47</i>	<i>-1.31</i>	<i>+0.45</i>	<i>+0.42</i>

Table 2: Magnitudes of the generalized strain energy density factor Σ for a notch perpendicular to the interface ($\phi = 90^\circ$) calculated purely from the GSIFs and also accounting for both GSIF and T-stress. In italics are the angles of the crack propagation into the material of substrate. Dimensions: Σ [N/m], r_0 [mm]

Now, compare the values obtained using both singular and nonsingular fields, i.e. accounting for both the GSIFs and T-stress. We can clearly see that by increasing the ratio E_1/E_2 , the magnitudes of Σ also monotonously increase. In other words, the more compliant the material of substrate is in comparison to coating, the higher is the magnitude of Σ . The same numerical trend holds also for V-notches with $2\gamma > 0^\circ$. Apparently, in these cases it does not matter if one uses only the GSIFs or both the GSIF and T-stress.

The conclusions drawn from the obtained data have one very important physical interpretation. The larger is the generalized strain energy density factor Σ the less energy is required for the propagation to the target layer. Similarly, the smaller is Σ the greater energy is needed to keep the propagation process going. From this point of view the interface between two elastic materials can be regarded as a barrier to further growth of the defect when the Σ factor is small in comparison to its critical value Σ_C .

Furthermore, for the assessment of the stability of bimaterial V-notches with the notch angle $2\gamma > 0^\circ$, the only necessary stress terms are those that are singular with respect to the radial distance. The nonsingular stress field represented by the T-stress can be regarded as a correction that is, however, not necessary in determining the factor Σ . This is not the case for a sharp crack ($2\gamma = 0^\circ$) propagating from a stiff coating into a more compliant material of substrate, where both the singular and nonsingular stress terms are necessary.

Since the dimension of both Σ and Σ_C does not change with geometry of the V-notch, its

orientation and elastic mismatch at the interface, such comparison between Σ and Σ_C seems to be very worthy in the decision on the stability of the crack emanating from the V-notch tip. The critical value Σ_C can be essentially fitted from the experimental data and thus we can regard it as a material characteristic.

7.3 Inclined notch terminating at the interface

This analysis takes aim at the dependence of the fracture-mechanical parameters on the angle between the notch axis and interface. The modeled configuration as well as the angles used to describe the notch orientation are showed in Fig. 11. The same geometrical properties as in the previous analysis were used to compare the results obtained for a perpendicular and generally inclined V-notch. The external loading was again applied in the direction parallel to the interface and so the inclined notch was exposed to the general mixed-mode of loading.

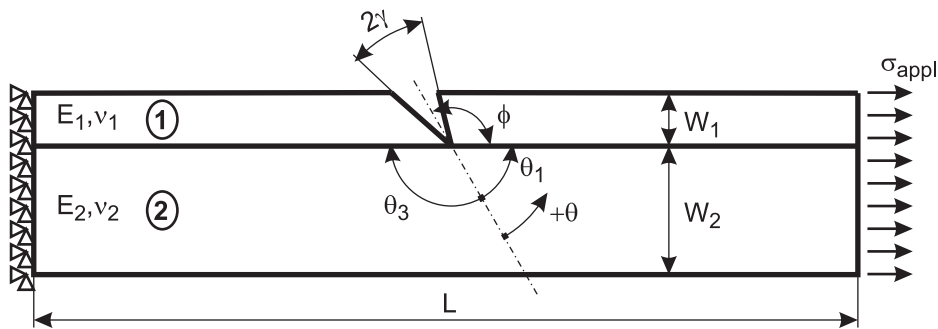


Figure 11: Model of an inclined notch terminating at the bimaterial interface.

From the data summarized in the Dissertation, one can clearly see that the orientation of the notch axis significantly influences both generalized stress intensity factors. From this perspective, some of the earlier studies that neglected the influence of the GSIF H_2 corresponding to the higher of the two eigenvalues in $0 < \lambda < 1$ essentially mathematically altered the physics of the problem. The error in the description of the real growth of a crack initiated at the V-notch tip must have increased with increasing magnitude of H_2 in those analyses.

Remember that from the knowledge of the GSIFs we cannot directly say whether or not the stress field for a particular geometrical configuration attains the critical state and the crack suddenly delaminates the uncracked layer. Instead, we again used the previously derived modification of the Sih's strain energy density criterion accounting for all the generalized stress intensity factors and also the T-stress. Similarly as in the last example, we were again interested in the quantification of the effect of the nonsingular stress term and deciding on the importance of this stress term in the prediction of unstable crack propagation.

Calculation of Σ at $r_0 = 0.01$ mm

The strain energy density factors Σ calculated at the radial distance $r_0 = 0.01$ mm are summarized in Tab. 3. One can clearly see that if the target layer is stiffer than coating, Σ is small and the substrate works as a barrier to further growth of the bimaterial defect. Conversely,

if the substrate is more compliant than coating, the interface accelerates the growth of the microcracks initiated at the V-notch tip.

Sih's modified strain energy density factor Σ calculated at $r_0 = 0.01$ mm

E_1/E_2	$2\gamma = 0^\circ$		$2\gamma = 30^\circ$		$2\gamma = 60^\circ$	
	$\Sigma(H_1, H_2)$	$\Sigma(H_1, H_2, T)$	$\Sigma(H_1, H_2)$	$\Sigma(H_1, H_2, T)$	$\Sigma(H_1, H_2)$	$\Sigma(H_1, H_2, T)$
0.5	53.97	52.32	51.01	51.37	44.09	44.30
0.6	114.20	111.32	108.04	108.07	91.14	91.40
1.0	306.59	304.82	299.41	299.26	251.70	251.93
1.5	533.88	532.33	519.99	519.00	447.74	447.73
2.0	744.02	746.12	733.60	733.47	649.15	649.32

Table 3: Magnitudes of the generalized strain energy density factor Σ for a notch inclined towards the interface ($\phi = 105^\circ$) calculated purely from the GSIFs and also accounting for both GSIF and T-stress. Dimensions: Σ [N/m]

Table 3 reveals an important feature of the model used in this analysis. Since the bimaterial crack/notch is inclined towards the interface, maximum value of the modified Sih's strain energy density factor corresponds always to crack. It practically means that a crack inclined towards the interface is more susceptible to brittle failure than the corresponding V-notch having the same angle with interface.

Calculation of Σ and θ_0 at the plastic zone boundary

In order to show the change in values of the strain energy density factor Σ , we also calculated the radii of the plastic region corresponding to yield stress $\sigma_0 = 350$ MPa. The magnitude of Σ determined at the plastic zone boundary is then regarded as the representative value of the strain energy density factor that characterizes the stability of the cracked model.

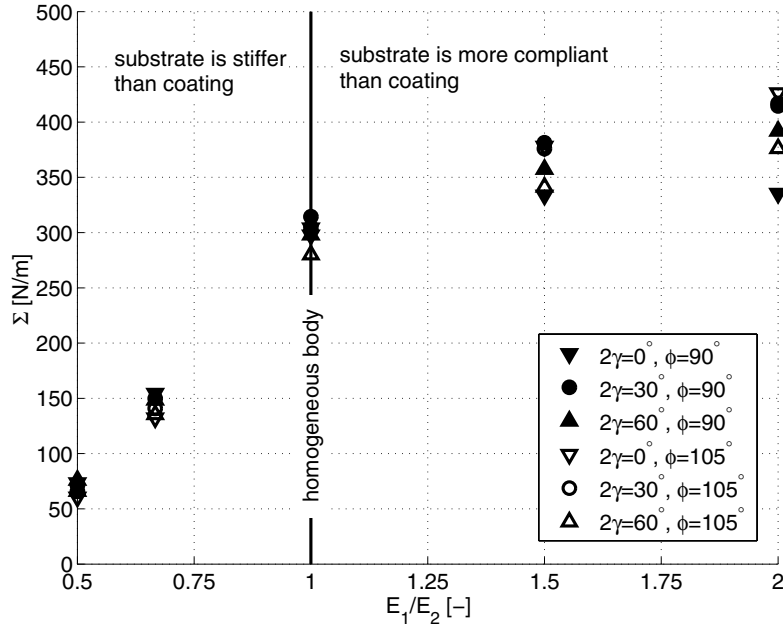


Figure 12: Variation of the factor Σ with the mismatch of the elastic moduli.

It is apparent that the results do not have so convincing trend as in the case of a notch perpendicular to the interface. Comparing the data in each column, one can immediately see that the factor monotonously increases with increasing ratio E_1/E_2 , which is in agreement with our expectations. Furthermore, the magnitudes of Σ for $E_1/E_2 > 1$ decrease with opening of the V-notch. V-notches with larger openings are therefore, according to this model, less susceptible to brittle failure than sharper notches.

Sih's modified strain energy density factor Σ calculated at the plastic zone boundary						
E_1/E_2	$2\gamma = 0^\circ$		$2\gamma = 30^\circ$		$2\gamma = 60^\circ$	
	$\Sigma(H)$	$\Sigma(H, T)$	$\Sigma(H_1, H_2)$	$\Sigma(H_1, H_2, T)$	$\Sigma(H_1, H_2)$	$\Sigma(H_1, H_2, T)$
	$\theta_0(H)$	$\theta_0(H, T)$	$\theta_0(H_1, H_2)$	$\theta_0(H_1, H_2, T)$	$\theta_0(H_1, H_2)$	$\theta_0(H_1, H_2, T)$
	$r_0 = 0.033$		$r_0 = 0.046$		$r_0 = 0.066$	
0.5	63.29	60.41	64.76	65.88	65.21	65.91
	<i>-15.62</i>	<i>-15.59</i>	<i>-11.93</i>	<i>-12.12</i>	<i>-7.54</i>	<i>-7.62</i>
	$r_0 = 0.131$		$r_0 = 0.150$		$r_0 = 0.176$	
0.6	141.48	132.04	139.90	141.01	133.87	135.42
	<i>-17.09</i>	<i>-17.39</i>	<i>-14.59</i>	<i>-14.74</i>	<i>-9.92</i>	<i>-10.03</i>
	$r_0 = 0.281$		$r_0 = 0.302$		$r_0 = 0.328$	
1.0	306.60	297.67	305.60	304.73	278.80	280.04
	<i>0.00</i>	<i>+1.43</i>	<i>-15.82</i>	<i>-13.96</i>	<i>-11.84</i>	<i>-11.41</i>
	$r_0 = 0.410$		$r_0 = 0.430$		$r_0 = 0.453$	
1.5	386.62	377.95	381.26	375.96	341.28	341.26
	<i>-14.45</i>	<i>-14.76</i>	<i>-15.20</i>	<i>-15.38</i>	<i>-13.01</i>	<i>-13.03</i>
	$r_0 = 0.484$		$r_0 = 0.503$		$r_0 = 0.525$	
2.0	414.59	426.29	417.58	416.85	375.28	376.15
	<i>-12.57</i>	<i>-12.07</i>	<i>-13.89</i>	<i>-13.92</i>	<i>-13.30</i>	<i>-13.20</i>

Table 4: Magnitudes of the generalized strain energy density factor Σ for a notch inclined towards the interface ($\phi = 105^\circ$) calculated purely from the GSIFs and also accounting for both GSIF and T-stress. In italics are the angles of the crack propagation into the material of substrate. Dimensions: Σ [N/m], r_0 [mm]

This statement is strictly valid only in the case, when both the singular and nonsingular stress terms are used in the analysis. Neglecting the effect of T-stress, one can see that for $2\gamma = 0^\circ$ and $E_1/E_2 = 2$, the factor Σ is smaller than that for the corresponding notch with angle $2\gamma = 30^\circ$. Since this discrepancy is associated only with crack, we assume that the T-stress should be included in the description of the stress field around such bimaterial cracks. Variation of the factor Σ with the ratio E_1/E_2 is plotted in Fig. 12; the values of Σ were calculated using both GSIFs and T-stress at the plastic zone boundary.

When analyzing the crack propagation angles written in Tab. 4, remember that the angle θ_0 is measured from the direction of the notch axis. Since the notch is now inclined 15° from the normal to the interface, crack propagation direction $\theta_0 = -15^\circ$ essentially means that the further propagation is assumed in the direction perpendicular to the interface. From the experimental measurements, the crack propagating from a compliant coating into a stiffer substrate feels a resistance that deflects the crack towards the direction of interface. On the other hand, once the crack initiates in the stiffer material and propagates further into the more compliant substrate, the crack is accelerated by the interface and propagates perpendicularly to the maximum applied stress.

8 CONCLUSION

The analytical description of the stress field around a generally oriented V-notch terminating at interface between two elastic materials was investigated. Because the stress field is not uniquely determined, but depends on the amplitude of the stress field corresponding to every eigenvalue, it was crucial to introduce a sufficiently accurate numerical procedure for the quantification of such parameters.

To achieve this goal, the interface was assumed to be perfectly bonded with continuous displacements and equivalence of tractions along the interface. Providing that both materials exhibit brittle behavior, the linear-elastic BEM was used to determine the stress and displacement field around the V-notch tip. Subsequently the generalized stress intensity factors and T-stresses were quantified using the contour integral method and direct extrapolation method.

To show the efficiency and accuracy of the integral method, three distinctive configurations of a notch in homogeneous as well as inhomogeneous body were modeled. The results obtained from the proposed methods were partly compared with our early work based on the direct extrapolation method and partly compared with the improved direct extrapolation technique derived in this Dissertation. The direct method strongly depends on the smoothness of the stress distribution within the chosen region and so its application to homogeneous bodies gives satisfactory results. In the case of steeper stress distribution ahead of the crack tip, it is sometimes difficult to find a linear section along which the stresses could be interpolated. The proposed integral method, on the other hand, yields a powerful mechanism for the quantification of the GSIF related to a specific eigenvalue λ .

To quantify the T-stress, another method based on the application of the interaction M-integral between two independent elastic states was introduced. The attempt to exceed this methodology also for the quantification of the T-stress in cracked bimetals was not successful, because the analytical expression of the auxiliary field that would satisfy the conditions of continuity of the displacement derivatives across the nonhomogeneous interface was not found.

Comparison of the actual stress state in the cracked bimaterial with the critical state was done using the modified Sih's strain energy density concept accounting for the effect of all singular stress terms and also nonsingular stress field. The reason for considering the latter was a belief that it can play an important role in the stability of the general bimaterial V-notches. Validity of such a consideration was tested on several examples by comparing the corresponding values of the modified Sih's factor Σ .

The methods for the calculation of the fracture-mechanical parameters were successfully used for the assessment of the stability of bimaterial V-notches. It was proven that the dominant role in the description of the stability of the bimaterial V-notches with nonzero opening angle and arbitrarily oriented towards the interface, is played by the singular stress terms. On the other hand, in the case of bimaterial cracks, the stability estimates are generally more accurate if the effect of the T-stress is taken into account. By comparing the intrinsic value of the modified strain energy density factor Σ with its critical value Σ_C , one can directly conclude on the stability of the layered structures weakened by bimaterial cracks or V-notches.

Finally, the concepts and discussions involved in this work form a fundamental set of knowledge required for a more sophisticated design of structural components made of brittle materials, like PMMA, composite laminates, welded joints, etc. However, the experimental verification of the results presented in this Dissertation is necessary to fully justify the underlying continuum approach.

REFERENCES

- [1] Balaš, J., Sládek, J., Sládek, V.: Stress Analysis by Boundary Element Methods, *Elsevier*, Amsterdam, 1989
- [2] Beer, G.: Programming the Boundary Element Method. An introduction for Engineers, *J. Wiley & Sons*, Chichester, Great Britain, 2001
- [3] Bogy, D.B.: On the plane elastostatic problem of a loaded crack terminating at a material interface, *Journal of Applied Mechanics*, ASME 71-APM-0, 1971
- [4] De Hosson, J. Th. M., Zhou, X. B., Van den Burg, M.: Structure-property relationship of metal-ceramic interfaces produced by laser processing, *Mat. Res. Soc. Symp. Proc.*, Vol. **319**, pp. 21–32, 1994
- [5] Fenner, D. N.: Stress singularities in composite materials with an arbitrarily oriented crack meeting an interface, *Int. Journal of Fracture*, Vol. **12**, No. 5, pp. 705–721, 1976
- [6] Holzmann, M.: Současný stav hodnocení lomové houževnatosti v tranzitní oblasti ("master" křivka, $J_C - Q$ diagram), *seminar Brittle Fracture*, Institute of Physics of Materials, Academy of Sciences of the Czech Rep., Brno, 1998 (in Czech)
- [7] Im, S., Kim, K.-S.: An application of two-state M-integral for computing the stress intensity of the singular near-tip field for a generic wedge, *Journal of Mechanics and Physics of Solids*, Vol. **48**, pp. 129–151, 2000
- [8] Klusák, J., Knésl, Z.: Evaluation of threshold values for the propagation of a fatigue crack starting at a V-notch, *Conference Numerical Methods in Continuum Mechanics*, Liptovský Ján, Slovakia, 2000
- [9] Knésl, Z.: The application of the strain energy density concept to the determination of a crack propagation direction initiated at a sharp notch tip, *Acta Technica ČSAV*, Vol. **38**, pp. 221–234, 1993
- [10] Leevers, P. S., Radon, J. C.: Inherent stress biaxiality in various fracture specimen geometries, *Int. J. of Fracture*, Vol. **19**, pp. 311–325, 1982
- [11] Mukherjee, S.: CPV and HFP integrals and their applications in the boundary element method, *Int. J. of Solids and Structures*, Vol. **37**, pp. 6623–6634, 2000
- [12] Náhlík, L.: Šíření únavových trhlin v okolí rozhraní dvou elastických materiálů, *Ph.D. Dissertation*, Institute of Solid Mechanics, Brno University of Technology, Czech Republic, 2001 (in Czech)
- [13] Qian, Z. Q., Akisanya, A. R.: Wedge corner stress behaviour of bonded dissimilar materials, *Theor. and Appl. Fracture Mechanics*, Vol. **32**, pp. 209–222, 1999
- [14] Sinclair, G. B., Okajima, M., Griffin, J. H.: Path independent integrals for computing stress intensity factors at sharp notches in elastic plates, *Int. J. of Numerical Methods in Engineering*, Vol. **20**, pp. 999–1008, 1984
- [15] Sládek, J., Sládek, V.: Evaluations of the T-stress for interface cracks by the boundary element method, *Eng. Fracture Mechanics*, Vol. **56**, No. 6, pp. 813–825, 1997
- [16] Sládek, V., Sládek, J.: Elimination of the boundary layer effect in BEM computation of stresses, *Communications in Appl. Num. Meth.*, Vol. **7**, pp. 539–550, 1991
- [17] Timoshenko, S., Goodier, J. N.: Theory of elasticity, 2nd Edition, *McGraw-Hill*, Tokyo, 1951

AUTHOR'S CURRICULUM VITAE

Department of Materials Science and Engineering
University of Pennsylvania
3231 Walnut Street
Philadelphia, PA 19104
U.S.A.

e-mail: groger@seas.upenn.edu
phone: +1-215-898-9171
fax: +1-215-573-2128



EDUCATION

University of Pennsylvania, Department of Materials Science and Engineering, U.S.A. (ongoing)
Doctor of Philosophy (Ph.D.) in Materials Science, advisor: Prof. Václav Vitek
Concentration: Atomistic modeling of the non-Schmid behavior of dislocations in bcc transition metals, Thermally activated dislocation motion in bcc single crystals and random polycrystals.

Brno University of Technology, Institute of Solid Mechanics (FME), Czech Rep. 2003
Doctor of Philosophy (Ph.D.) in Engineering Mechanics, advisor: Prof. Zdeněk Knésl
Concentration: Fracture mechanics of general stress concentrators, Boundary Element Methods.
Dissertation: Characterization of fracture-mechanical behavior of bimaterial V-notches using BEM

Slovak Academy of Sciences, Institute of Construction and Architecture, Slovakia 2001
Visiting scholar, advisor: Prof. Ján Sládek
Concentration: Fundamentals of the Boundary Element Methods, Singular integrals and methods of regularization of hypersingular kernels, Contour integrals for calculation of the stress intensity factors and T-stresses in linear-elastic fracture mechanics.

Brno University of Technology, Institute of Solid Mechanics (FME), Czech Rep. 1999
Inženýr (M.S. equivalent) in Engineering Mechanics, advisor: Dr. Zdeněk Florian
Master's thesis: Two-parameter fracture mechanics: Calculation of the Q-factor using FEM

Tampere University of Technology, Applied Mechanics (DME), Finland 1998
Study visit, advisor: Prof. Juhani Koski
Concentration: The Finite Element Method, Fracture Mechanics, Applied Computer Programming

TEACHING/RESEARCH EXPERIENCE

Cooperative researcher, Institute of Physics of Materials, AS of the Czech Republic 2000-02
Lecturer, Strength of Materials II., Brno University of Technology, Brno 2000-02

HONORS AND GRANTS

Dean's award, competition of Ph.D. works, 5th place, Brno University of Technology 2001
Rector's award, Brno University of Technology 1999
M.S. diploma with honors, Faculty of Mechanical Engineering, Brno Univ. of Technology 1999

LANGUAGES AND COMPUTERS

Czech: *mother tongue*, English: *fluent*, Russian: *intermediate*
Computers: Matlab, ANSYS parametric design language, C/C++, Pascal, L^AT_EX, Linux.